LIMNOLOGY and OCEANOGRAPHY

ASLO

Limnol. Oceanogr. 68, 2023, S39–S53

doi: 10.1002/lno.12192

Effects of Atlantification and changing sea-ice dynamics on zooplankton community structure and carbon flux between 2000 and 2016 in the eastern Fram Strait

Simon Ramondenc [1,2*] Eva-Maria Nöthig [1] Lili Hufnagel [2] Eduard Bauerfeind [1] Kathrin Busch [3] Nadine Knüppel [1] Angelina Kraft [1,4] Franz Schröter [1] Miriam Seifert [1] Morten H. Iversen [1,2*]

[1]Alfred Wegener Institute for Polar and Marine Research, Bremerhaven, Germany
[2]MARUM, Center for Marine Environmental Sciences, University of Bremen, Bremen, Germany
[3]GEOMAR Helmholtz Centre for Ocean Research Kiel, Kiel, Germany
[4]Technische Informationsbibliothek, Hannover, Germany

Abstract

The collection of zooplankton swimmers and sinkers in time-series sediment traps provides unique insight into year-round and interannual trends in zooplankton population dynamics. These samples are particularly valuable in remote and difficult to access areas such as the Arctic Ocean, where samples from the ice-covered season are rare. In the present study, we investigated zooplankton composition based on swimmers and sinkers collected by sediment traps at water depths of 180–280, 800–1320, and 2320–2550 m, over a period of 16 yr (2000–2016) at the Long-Term Ecological Research observatory HAUSGARTEN located in the eastern Fram Strait (79°N, 4°E). The time-series data showed seasonal and interannual trends within the dominant zooplankton groups including copepoda, foraminifera, ostracoda, amphipoda, pteropoda, and chaetognatha. Amphipoda and copepoda dominated the abundance of swimmers while pteropoda and foraminifera were the most important sinkers. Although the seasonal occurrence of these groups was relatively consistent between years, there were notable interannual variations in abundance, suggesting the influence of various environmental conditions such as sea-ice dynamic and lateral advection of water masses, for example, meltwater and Atlantic water. Statistical analyses revealed a correlation between the Arctic dipole climatic index and sea-ice dynamics (i.e., ice coverage and concentration), as well as the importance of the distance from the ice edge on swimmer composition patterns and carbon export.

The Arctic is currently showing rapid climate change in all environments including the ocean, cryosphere, land, and atmosphere (Elmendorf et al. 2012; Carmack et al. 2015). The Arctic Ocean has experienced a larger impact from global warming than regions at mid-latitudes (Pörtner et al. 2019) showing that this area is more sensitive to climatic changes than other oceanic regions (Comiso et al. 2008). This stronger subjection to warming in the Arctic is known as Arctic Amplification. The Arctic Amplification is driven by a recent warming of the Atlantic water inflow through the Barents Sea (Loeng 1991) and via the West Spitzbergen Current where Atlantic water is transported poleward through the Fram Strait along the west coast of Svalbard (Aagaard et al. 1987). The recent warming due to Atlantic inflow water and resulting retreat of ice-cover is termed Atlantification of the Arctic Ocean (Polyakov et al. 2017). Atlantification is part of the borealization of the Arctic Ocean (Polyakov et al. 2020) and refers both to the poleward extension of Atlantic water and to the increasing fraction of the water column occupied by Atlantic water. A recent study has shown that the Fram Strait has been affected by Atlantification since the early 20th century (Tesi et al. 2021), resulting in significant reduction in sea-ice extent with a sea-ice loss rate of 4.1% per decade (Cavalieri and

*Correspondence: simon.ramondenc@awi.de; morten.iversen@awi.de

Author Contribution Statement: S.R. wrote the paper together with E.-M.N., L.H., and M.H.I. E.B., K.B, A.K., N.K., M.S., and F.S. provided, respectively, delivered considerable amounts of counting data to the manuscript, as well as picked zooplankton for hours during many months or even years. All authors were involved in the discussion about the long-term perspective of environmental change in the Arctic Ocean. All authors revised and approved the manuscript.

Special Issue: Cascading, Interactive, and Indirect Effects of Climate Change on Aquatic Communities, Habitats, and Ecosystems. *Edited by: Susanne Menden-Deuer, Maarten Boersma, Hans-Peter Grossart, Ryan Sponseller, Sarah A. Woodin and Deputy Editors Julia C. Mullarney, Steeve Comeau, and Elisa Schaum.*

Parkinson 2012) and a decrease in sea-ice thickness of 0.58 m per decade over the period 2000–2012 (Lindsay and Schweiger 2015). As a result of ice-melt in the Central Arctic Ocean, the volume of sea-ice export through the Fram Strait has increased by 10% per decade from 1990 to 2010 (Zamani et al. 2019). It is evident that the climate-driven changes for the Arctic Ocean are already impacting the ecosystem at both microbial (Comeau et al. 2011) and higher trophic levels, including alterations in fish distribution and migration (Fossheim et al. 2015), and reduction in ice-dependent mammals habitats (Descamps et al. 2017).

The Arctic Ocean and the Fram Strait are both remote and either permanently or seasonally ice-covered making access to the area difficult year-round. Consequently, this area is largely understudied, especially during the polar night. Though long-term chemical, physical, and biogeochemical time series have been successfully collected by ocean observatories (Soltwedel et al. 2016), it is still difficult to continuously sample plankton organisms. This is especially true for zooplankton, which have evolved to exhibit escape behavior when they perceive hydromechanical disturbances (Kiørboe and Visser 1999), such as those created by the inflow of sampling pumps. At present, multiyear sampling of zooplankton in the Arctic Open Ocean and the northern Fram Strait is primarily limited to summer when research vessels can access these regions (Nöthig et al. 2015).

Several hydroclimatic indices such as North Atlantic Oscillation and Arctic Oscillation exert a significant control on climatic parameters that perturb North-Atlantic and Arctic marine ecosystems (Dickson et al. 2000). The connections between large-scale hydroclimatic oscillations and zooplankton communities have been recognized for a long time in the North Atlantic Ocean (Fromentin and Planque 1996). However, it is still unclear how these large-scale hydroclimatic indices affect environmental conditions in the Arctic or in the Fram Strait (i.e., ice flux through the Fram Strait, warm Atlantic inflow into the Arctic Ocean; Dickson et al. 2000) even if the principal changes in Arctic sea-ice phenology appear to be predominantly atmospherically driven (Barber et al. 2015).

Here, we investigate changes in export flux and zooplankton community structure from existing sediment trap data from the period between 2000 and 2016. Data were collected at a monthly to weekly resolution across different seasons and depths. Zooplankton may enter sediment traps by passively sinking (sinkers) or by actively swimming into the trap (swimmers; Knauer et al. 1979) where they are preserved by a fixative. Typically, only sinkers are considered to be part of the export flux while swimmers are considered as a contamination and removed prior to biogeochemical analyses (Michaels et al. 1990). However, sediment traps offer long time series of zooplankton swimmers and sinkers that can be used as proxies and allow seasonal sampling that would not be possible with net sampling due to the difficulties in accessing the polar regions by ship year-round, especially during the ice-covered seasons. Previous studies used information on the abundance and composition of sinkers and swimmers to investigate, for instance, correlations between zooplankton communities and environmental variables (Makabe et al. 2010), relationships between zooplankton and water masses (Willis et al. 2006), as well as identified patterns in vertical migration of the zooplankton (Tokuhiro et al. 2019). Several ocean observatories have sediment trap time series spanning several decades, which can offer a window into how past climate change has induced alterations and shifts in zooplankton communities.

In this context, the aim of this study was to use zooplankton collections from sediment traps moored at the central station of the HAUSGARTEN Long-Term Ecological Research (LTER; at station HG-IV [∼79°N; 4°E]) observatory from the period between 2000 and 2016 to identify changes in zooplankton composition, seasonality, and relative abundance. By linking these changes to biological, physical, and sea-ice observations from long-term deployed sensors and remote satellite observations, we evaluated how climate change in the eastern Fram Strait might have impacted the zooplankton communities and export flux.

Materials and methods

Study area

The Fram Strait is a very dynamic region in terms of water mass exchange, eddy formation, and fluctuating sea-ice conditions (Maslowski et al. 2004). Two strong opposing currents create the Arctic Polar Front (Fig. 1): (i) the warm and salty Atlantic water, the West Spitsbergen Current, flows northwards to the Arctic Ocean along the west coast of Spitsbergen; and (ii) the cold and less salty Arctic water, the East Greenland Current, flows from the Arctic toward the south along the Greenlandic east coast. The Fram Strait acts as a corridor between the Arctic and the Atlantic Oceans with both seasonal and annual variations in the amount of water inflow and outflow (Beszczynska-Möller et al. 2012). The annual net water volume transport through the Fram Strait has been estimated to be 4.2 Sv with an average flow of around 9.5 and 13.7 Sv for the northward and southward directions, respectively (Fahrbach et al. 2001; Beszczynska-Möller et al. 2012). During the past decades, two "warm anomaly" periods were observed (1999–2000 and 2005–2007) as a result of an increased inflow of warm Atlantic water into the Fram Strait (Beszczynska-Möller et al. 2012). The last warm event (2005–2007) was associated with stronger geostrophic winds and increased sea-ice melting west and north of Svalbard, which caused an increase in ice export to the Fram Strait where the warm conditions caused high melting and overall induced the decline in ice cover in the Fram Strait (Smedsrud et al. 2011; Lalande et al. 2013).

Sediment trap collection

The mooring was situated at the central station (HG-IV; 79°01N, 4°20E) of the Long-Term Ecological Research observatory HAUSGARTEN that is operated by the Alfred Wegener

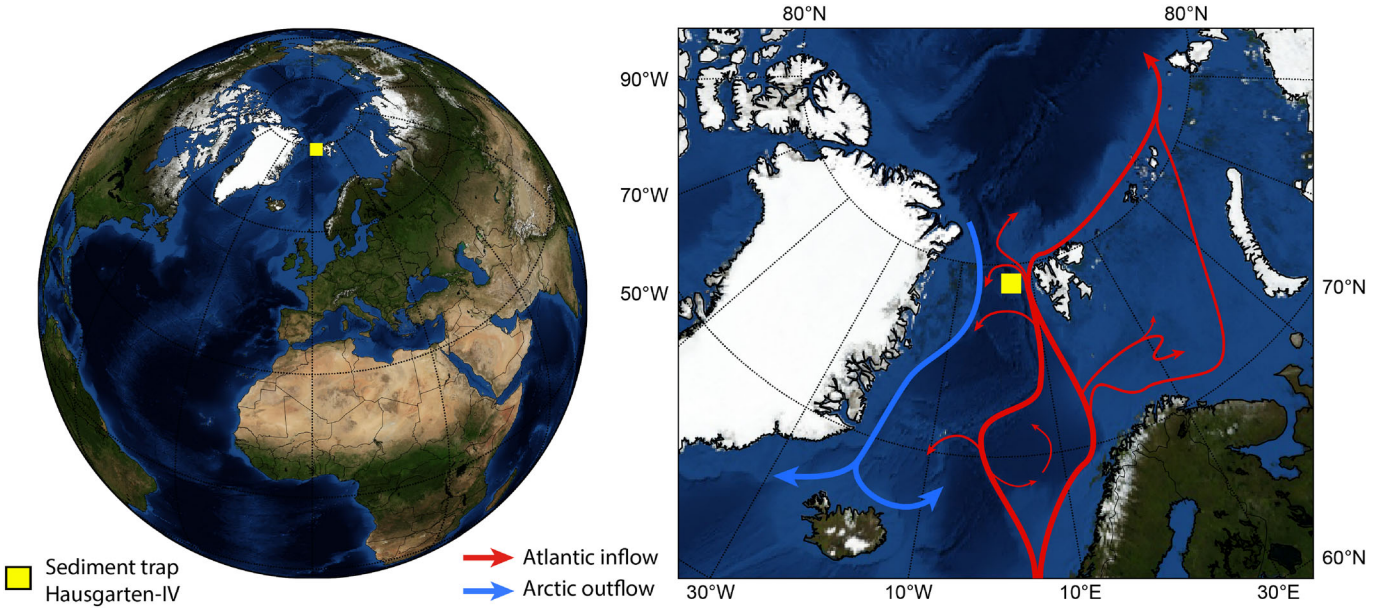

Fig. 1. Oceanographic setting in the area of the central HAUSGARTEN (HG-IV [4°E; 79°N]; yellow square) long-term mooring site with the surface warm Atlantic (red arrows) and cold Arctic water masses (blue arrows) trajectories.

Institute (Fig. 1; Table 1). Kiel type sediment traps (K.U.M. trap type K/MT 234) were moored and exchanged annually in the eastern Fram Strait between 2000 and 2016. Before 2004, two different water depths were sampled (180–280 m, 2320–2550 m; Table 1) and from 2004, a middle trap was added to the mooring system (800–1320 m; Table 1). Due to instrument failure, not all traps at all depths collected material (hence, no deep trap samples are available for 2000–2002 and from 2001 to 2002 the shallow traps only sampled until February. From 2004 to 2005, there were no deep trap samples, from 2003 to 2004, the shallow and deep traps did not sample and the intermediate trap did not sample from 2008 to 2009). From 2012 to 2016, the material collected in the middle traps has not been analyzed yet due to time limitation. In addition, this study does not include the measurements performed by the upper sediment trap between July 2009 to July 2010 since it was moored at a shallower depth ($\sim$ 80 m) than during all other collection periods.

Prior to each deployment, the sampling cups on the sediment traps were filled with filtered seawater adjusted to a salinity of 40 psu with NaCl and poisoned with mercury chloride ($HgCl_2$: final solution of 0.14%) to preserve the collected material in the sampling cups during deployment and after recovery. After collection, samples were refrigerated at 4°C and stored in the dark. Before biogeochemical analysis, zooplankton larger than 0.5 mm was picked individually using soft forceps, gently rinsed with filtered seawater, and identified and counted under a dissecting microscope (Olympus SZX10; X20-50 magnification). The zooplankton organisms were grouped and enumerated over the entire sampling period into four swimmer groups, copepoda, ostracoda, amphipoda, chaetognatha, and two sinker groups, pteropoda and foraminifera. The distribution of zooplankton groups according to swimmer or sinker categories has been done based on ecological traits (i.e., swimming ability) of individuals and the "freshness," that is, were they still having their organic matter and did not look degraded. Unfortunately, foraminifera were only counted since 2007 for the deep trap and from 2010 to 2016 for the upper and middle traps. The taxonomic level was kept at general groups since we only had species identifications for pteropoda and amphipoda during some periods throughout the time series. All pteropoda counted were treated as one group of sinkers, in contrast to Bauerfeind et al. (2014) and Busch et al. (2015), where pteropoda were divided into swimmers that still contain body tissue parts and sinkers that were empty shells. To be able to compare seasonal and interannual differences in zooplankton composition, the flux of each group was calculated as:

$$\mathrm{Flux}\left(\mathrm{ind.\ m^{-2}\,d^{-1}}\right) = \frac{\mathrm{Tot_{group}} \times A_{\mathrm{collection}}}{t_{\mathrm{collection}}},$$

where $\mathrm{Tot_{group}}$ is the total number of zooplankton counted within a group, $t_{\mathrm{collection}}$ is the collection time in days for each individual sampling cup, and $A_{\mathrm{collection}}$ is the area of the trap opening (0.5 $\mathrm{m^{-2}}$). For illustration, the fluxes were sorted as monthly flux:

$$\mathrm{Flux_{monthly}} = \frac{\mathrm{Total\ flux_{month}}}{\mathrm{Nb\,day_{month}}} = \sum_{i=1}^{n} \frac{[\mathrm{day\_trap}_i \times \mathrm{Flux}]}{\mathrm{day\_trap}_i},$$

where n and day_trap represent the number of collection cups that were open during 1 month and the number of sampling

Table 1. Mooring name, sampling period, mooring position, trap deployment depths, and number of samples (i.e., sediment trap collection cup) obtained by respective traps deployed at the central station of the LTER observatory HAUSGARTEN of the Alfred Wegener Institute.

Mooring	Sampling time (start–end)	Lat N	Long E	Trap depth (m)	*n*
FEVI1	31 Aug 2000–14 Aug 2001	79°01.70	4°20.86	280*	16
FEVI2	14 Aug 2001–29 Jul 2002	79°01.50	4°21.30	280*	15
FEVI3	14. Aug 2002–10 Jun 2003	79°01.04	4°19.77	280	20
FEVI7	12 Jul 2004–19 Aug 2005	79°00.99	4°20.62	280*	17
				800	20
FEVI10	23 Aug 2005–31 Aug 2006	79°01.00	4°20.62	179*	17
				1230	16
				2357	16
FEVI13	25 Aug 2006–20 Jun 2007	79°00.82	4°20.50	230*	19
				1300	20
FEVI16	21 Jul 2007–15 Jul 2008	79°00.82	4°20.62	190*	19
				1316	20
				2370	20
FEVI18	17 Jul 2008–18 Jul 2009	79°00.40	4°20.0	196*	20
				2372	19
FEVI20	20 Jul 2009–15 Jul 2010	79°00.43	4°20.05	2550	20
FEVI22	10 Jul 2010–30 Jun 2011	79°00.41	4°19.90	200*	20
				1250	20
				2495	20
FEVI24	29 Jul 2011–16 Jul 2012	79°00.42	4°19.90	200*	19
				1225	20
				2495	20
FEVI26	25 Jul 2012–08 Jul 2013	79°00.43	4°19.78	205*	20
				2356	20
FEVI28	10 Jul 2013–15 Jun 2014	79°03.76	4°19.81	205	17
				2341	12
FEVI30	24 Jun 2014–15 Jul 2015	79°00.24	4°19.81	213	20
				2319	20
FEVI32	14 Aug 2015–20 Jun 2016	79°00.43	4°19.92	205	18
				2341	18

*The swimmers and sinkers samples available to be coupled with the environmental measurements (biogeochemical fluxes, physical oceanographic measurements, hydroclimatic indices).

days each cup was open, respectively. All swimmer and sinker data are available on PANGAEA website. In addition to zooplankton flux, biogeochemical measurements for total particulate matter flux, particulate organic carbon (POC), particulate organic nitrogen (PON), biogenic silica (bPSi), total calcium carbonate ($CaCO_3$; calcite and pteropoda aragonite), and carbon and nitrogen isotopes ($\partial^{13}C$ and $\partial^{15}N$) were analyzed. These measurements were available from 2000 to 2012 for the upper traps. A detailed description of the biogeochemical analyses is provided by Lalande et al. (2013, 2016) and by Bauerfeind et al. (2009).

Environmental parameters and climate indices

Physical oceanographic variables were recorded hourly at the same area and period as the sediment trap mooring and included measurements of temperature, salinity, current direction, and current velocity for the upper 150 m of the water column (*see* 10.1594/PANGAEA.900883; de Steur et al. 2009; Beszczynska-Möller et al. 2012). In addition, daily sea-ice coverage, atmospheric temperature, wind speed, and wind direction were available for the area between 2000 and 2016 (10.1594/PANGAEA.878244). Daily estimates of sea-ice concentration were generated using the NASA Team algorithm (Cavalieri et al. 1996) and mapped to a 25 × 25 km grid, which were downloaded from NSIDC/NOAA (http://nsidc.org/data/nsidc-0051). This data set was derived from brightness temperature data generated from Scanning Multichannel Microwave Radiometer and Sensor Microwave Imager and Sounder, respectively, on-board the Nimbus-7 satellite and the Defense Meteorological Satellite Program. To evaluate the impact of the sea-ice concentration on the sediment trap fluxes at HG-IV station, the closest daily

distances between the sea-ice edge (i.e., > 15% of sea-ice concentration) and the HG-IV station were estimated by interpolating raw data and measuring the distance from geographical coordinates.

We investigated the relative contribution of four large-scale hydroclimatic indices as potential indicators for sea-ice dynamics and the intrusion of Atlantic vs. Arctic waters into the Fram Strait:

i. The North Atlantic Oscillation (NAO) index describes the difference in pressure between Portugal (Lisbon) and Iceland (Reykjavik). During positive periods, there are large pressure differences between Europe and Iceland, and the Westerlies are shifted northward (Hurrell 1995). The changes of the NAO are affecting both the water mass movement and the biological production in the North Atlantic (Dickson et al. 2000).
ii. The Atlantic Multidecadal Oscillation (AMO) index is based on average sea surface temperature (SST) anomalies in the North Atlantic (0°–70°N) (Enfield et al. 2001). This index is positive when the North Atlantic Ocean is warmer than the southern part.

Monthly values of both large-scale hydro-climatic indices are available on the NOAA website: https://www.esrl.noaa.gov; https://www.cpc.ncep.noaa.gov.

In the Arctic, we focused specifically on the two leading modes in the sea-level pressure variability, the Arctic Oscillation and the Arctic Dipole. Both indices were derived from the National Centers for Environmental Prediction–National Center for Atmospheric Research reanalysis data (http://iridl.ldeo.columbia.edu/SOURCES/.NOAA/.NCEP-NCAR/.CDAS-1/.MONTHLY/), following the calculation method by Empirical Orthogonal Function (EOF) analysis of Wu et al. (2006).

iii. Arctic Oscillation is known as the principal mode of atmospheric circulation over the mid and high northern latitudes. The Arctic Oscillation positive phase keeps the cold Arctic air concentrated in the polar region by a counterclockwise jet stream at mid-latitude. In contrast, during the negative phase, this strong wind becomes weaker and unstable letting cold air escape to the south.
iv. The 2nd mode, identified as the Arctic Dipole, is the east–west dipole associated with a meridional wind and tends to affect the sea-ice transport from the central Arctic to the Atlantic Ocean via Fram Strait and the Transpolar Drift Stream. In this study, we define an Arctic Dipole positive phase as having a negative sea-level pressure anomaly over Greenland and a positive sea-level pressure over the Laptev Sea.

Statistical analyses

The upper sediment traps (180–280 m) provided the most complete record of swimmers and sinkers to study interannual and seasonal zooplankton variabilities. For each zooplankton group collected by the sediment traps the temporal changes were assessed by log transforming [$x' = \log(x + 1)$] their abundances. We present the data as log transformed values to give less weight to the sporadic events (e.g., zooplanktonic swarms) and, thereby, reduce outliers to make the patterns in the data more interpretable. For the same reasons, the 1st, 2nd (i.e., median), and 3rd quartiles are used to represent the total distributions and abundance of each swimmer and sinker group (Table 2). The trends were represented based on a heatmap and gaps in the time series were filled using Barnes interpolations ("oce" package in R; Kelley et al. 2018). The actual zooplankton abundances counted from each sediment trap sample were used as a proxy for the abundance of zooplankton in the water column. The collection of a specific zooplankton group shows that this group was present at the collection depth and period, but the absence of a group in the traps does not mean that the group was not present in the water column.

The degree of association between occurrence of zooplankton groups and environmental drivers were examined using ordination analyses. Mostly used in ecology, redundancy analysis (RDA) helps to understand the link between species distribution and environmental variables (Legendre and Legendre 2012) based on dimensionally homogeneous dataset. Raw data were

Table 2. Overall median zooplankton abundance (ind. m^{-2} d^{-1}) for the whole upper sediment trap time series and divided in seasonal median value; winter (January, February, and March), spring (April, May, and June), summer (July, August, and September), fall (October, November, and December).

Zooplankton groups	Winter	Spring	Summer	Fall	Range	1st quantile	2nd quantile (median)	3rd quantile
Pteropoda	2.9	0.1	2.0	4.8	0–1570	0.1	4.0	57.8
Foraminifera	0.1	1.0	4.9	0.7	0–3696	2.1	21.9	243.2
Copepoda	2.97	3.8	4.6	3.9	0–903	20.2	47.3	86
Ostracoda	2.0	1.9	3.0	2.6	0–107	4.6	8.7	18.2
Chaetognatha	0.6	2.1	0.5	0.0	0–124	0	0.4	4.2
Amphipoda	1.2	2.3	3.1	1.4	0–132	2.2	6.8	14.1
All	10.4	10.4	14.6	14.0	0–3843	72.9	132.8	303.23

grouped seasonally (winter: 21 December to 21 March; spring: 21 March to 21 June; summer: 21 June to 23 September; fall: 23 September to 21 December) for each year in order to maximize co-sampling with environmental variables (i.e., climatic indices, physical oceanographic and atmospheric variables, sea-ice condition, biogeochemical fluxes), and perform multivariate analysis. The RDA identified correlations between zooplankton abundance (response matrix) and environmental drivers (explanatory matrix). To avoid collinearity among factors, explanatory variables with variance inflation factor higher than 10 were eliminated.

Unfortunately, large sampling gaps interrupted the middle (800–1320 m) and deep (2320–2550 m) sediment trap time series, which complicated interannual zooplankton analyses. Nevertheless, these data sets were useful to describe the seasonal vertical distribution of organisms by comparing them with the upper trap collections.

All the statistical analyses and illustrations have been performed using Python (version 3.6.7) and R (version 3.5.1) computer programs.

Results

The time series included a total of 529 sample cups with 237, 116, and 176 cups in the upper, middle, and deep sediment traps, respectively. The zooplankton flux ranged from 0 to 3843 ind. m^{-2} d^{-1} with a median of 133 ind. m^{-2} d^{-1} for all upper traps throughout the whole time series (Table 2). Copepoda dominated the swimmers at all sediment trap depths (i.e., upper: 64%, middle: 75%, deep: 80% of the swimmers), while amphipoda, ostracoda, and chaetognatha were less abundant. From the upper sediment traps, the median copepoda abundance was 47 ind. m^{-2} d^{-1}, whereas in the middle and deep traps, the medians were only 11.7 and 1.5 ind. m^{-2} d^{-1}, respectively. In comparison, the most abundant sinkers were foraminifera in the upper, middle, and deep sediment traps (i.e., upper: 61%, middle: 89%, deep: 83% of the sinkers) with a median of 21, 112, and 187 ind. m^{-2} d^{-1}, respectively.

Interannual and seasonal variabilities of sinkers and swimmers in the upper sediment traps

Pteropoda and foraminifera

Pteropoda abundances ranged from 0 to 1570 ind. m^{-2} d^{-1} (Table 2) and their abundances were low during the 1st deployment (year 2000) and decreased to very low concentrations between 2002 and 2005 (Fig. 2a). From 2006 to 2011, abundances were increasing before reaching a high stable occurrence until 2016. Seasonality did not change interannually, and pteropoda exhibited a clear unimodal seasonal cycle with abundances decreasing from winter to summer with a peak during fall (Fig. 2a). As described in the "Materials and methods" section, the time series of foraminifera abundance was shorter than the others groups, which limited our discussion on the interannual changes. Briefly, their abundances increased from 2010 to 2013 and then decreased progressively until 2016 (data not shown). However, the foraminifera data were adequate to extract seasonal trends and showed high to low occurrences from summer to winter in the upper traps.

Copepoda

The number of copepoda ranged from 0 to 903 ind. m^{-2} d^{-1} within the entire sampling period (Table 2). Starting in 2000, the annual copepoda abundance was constant until 2002 whereas from 2003 to 2006 more copepoda were collected in the shallow sediment traps (Fig. 2b). In 2007, their abundance was similar to the 1st part of the time series but between 2008 and 2013 higher numbers of individuals were observed. From 2014 to 2016, the copepoda abundances showed a slight annual decrease. Interestingly, these interannual variations seemed to be associated with the seasonal occurrence where high copepoda abundances were observed during April to October/November between 2005–2006 and 2008–2013, while the rest of the time series showed high abundances between July and October/November (Fig. 2b).

Other zooplankton

We observed that the chaetognatha group had similar seasonal perturbations as those observed for copepoda (Fig. 2c). The chaetognatha abundance ranged from 0 to 124 ind. m^{-2} d^{-1} in the collected sediment trap samples (Table 2). The chaetognatha abundances increased during two successive periods between 2005 and 2006 and between 2008 and 2012 with peaks in abundance between March and September. For the remaining periods of the time series (i.e., from 2000 to 2004, 2007, and from 2013 to 2016), the peaks in chaetognatha abundances occurred between March and May (Fig. 2c). We did not observe any clear phenology for ostracoda throughout the entire time series (Fig. 2d), which showed a high monthly variability. The abundance of ostracoda ranged between 0 and 107 ind. m^{-2} d^{-1} (Table 2) with maximal values at the end of summer and beginning of fall (Fig. 2d). Interannual changes in the ostracoda abundance were observed during the slight decline between 2000 and 2007, as were changes in the seasonal patterns from a bimodal (spring and end summer peak) through 2005 to a unimodal distribution (peak end of summer) from 2005 to 2007. After 2007, the ostracoda abundance steadily increased until 2011 and consistently showed a gradual seasonal extension from spring to the end of summer. From 2013 to 2016, ostracoda were less abundant and showed a single reduced peak during late summer (Fig. 2d). The seasonal variations of amphipoda mainly showed a unimodal distribution with a maximal average from spring to late summer/early autumn (Fig. 2e). The abundance of amphipoda ranged between 0 and 132 ind. m^{-2} d^{-1} (Table 2) and appeared to increase from 2000 to 2004 before reaching a minimum from 2005 to 2006. Then, between 2007 and 2016, amphipoda had higher abundances with some fluctuations and maximum in 2008 and 2012 (Fig. 2e).

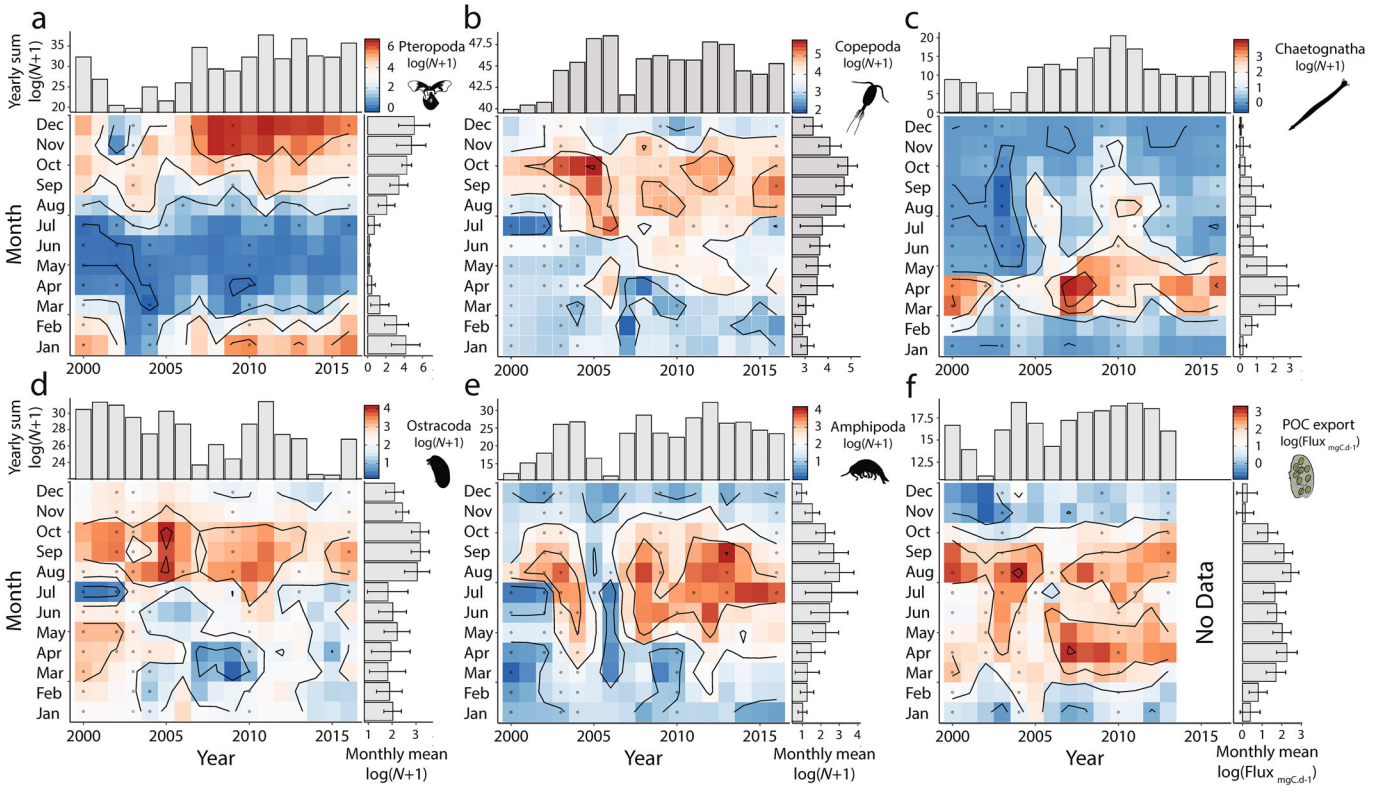

Fig. 2. Monthly mean of the log-transformed abundance of the five dominant swimmers/sinkers groups (pteropoda (**a**), copepoda (**b**), chaetognatha (**c**), ostracoda (**d**), amphipoda (**e**)) and POC flux (**f**) measured in the upper sediment traps over the time series. Squares with dots, vertical and horizontal bars charts represent, respectively, the period without data interpolated by Barnes method (cf. "Materials and methods" section), the monthly mean and annual sum of the zooplankton abundances.

Environmental drivers and biogeochemical fluxes associated to zooplankton recorded in the upper sediment traps

The RDA from the upper sediment traps showed that the percentages of accumulated constrained eigenvalues of the two canonical axes explained 49% of the total variance (Fig. 3; p-value < 0.01 and R^2 adj = 0.64). The 1st axis represented 42% of the overall variability and was mainly driven by the $CaCO_3$ flux, while the 2nd axis was primarily temperature driven and explained only 7% of the variability in the data (Fig. 3). The RDA sample scores in the reduced dimension were distributed seasonally, which indicated that the main variability in the dataset was linked to the seasonal variations and not to interannual variations.

The scaling 2-triplot confirmed that pteropoda were most abundant during fall and, as might be expected, demonstrated that they were positively correlated to the $CaCO_3$ flux. On the other hand, chaetognatha, and to a lesser extent amphipods, reached high abundances during spring. Both groups were positively correlated to ice concentration and POC flux, while they were negatively correlated to the distance from the sea-ice edge and Arctic Dipole index. The heatmap of POC flux (Fig. 2f) confirms the pattern observed in the multivariate analysis and highlights a bimodal distribution of carbon export in the Fram Strait with a maximum recorded in April and August. Interannual changes in POC flux were mainly caused by spring conditions, while the summer carbon export was annually stable (except in 2006). Copepoda and ostracoda were abundant during summer and positively correlated with AMO and wind direction, while both were negatively correlated with $\partial^{15}N$ (Fig. 3). In the warm years between 2005 and 2006, the non-summer seasons were grouped together with summer zooplankton clusters (i.e., fall 2005, winter 2006, and spring 2006), which may primarily be due to warmer water temperatures and high abundance of copepoda.

We correlated our observations to four large-scale hydro-climatic indices. Based on RDA, we found that Arctic Dipole was the main factor that explained the sea-ice dynamics (sea-ice concentration and distance to the trap station) in the Fram Strait. A positive Arctic Dipole pattern was correlated to increased marginal ice-zone distance to the HG-IV mooring and consequently also correlated to decreasing ice concentration in the HG-IV area. The 2nd leading EOF of annual-mean sea-level pressure anomalies (Fig. 4a) showed a clear east–west dipole. In addition, a strong linear relationship between ice

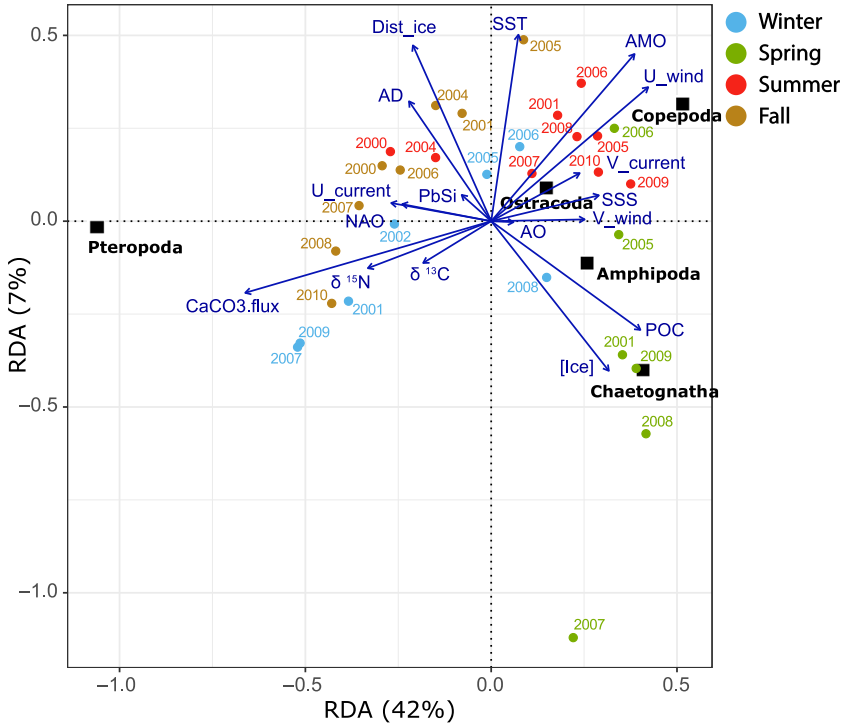

Fig. 3. RDA of Hellinger-transformed seasonal zooplankton data in the upper sediment traps constrained by several environmental variables (i.e., biogeochemical fluxes, hydroclimatic indices, and physical measurements). AD, Arctic Dipole; AMO, Atlantic Multidecadal Oscillation; AO, Arctic Oscillation; $CaCO_3$, Calcium carbonate flux; Dist_ice, ice distance between HG-IV and the sea-ice edge; [Ice], Ice concentration; NAO, North Atlantic Oscillation; PbSi, Particulate biogenic Silica; POC, Particulate Organic Carbon flux; SSS, Sea Surface Salinity; SST, Sea Surface Temperature; v_current/u_current, current direction; v_wind/u_wind, wind direction; $\partial^{15}N$ and $\partial^{13}C$ nitrogen and carbon isotopes, respectively, of particulate organic matter.

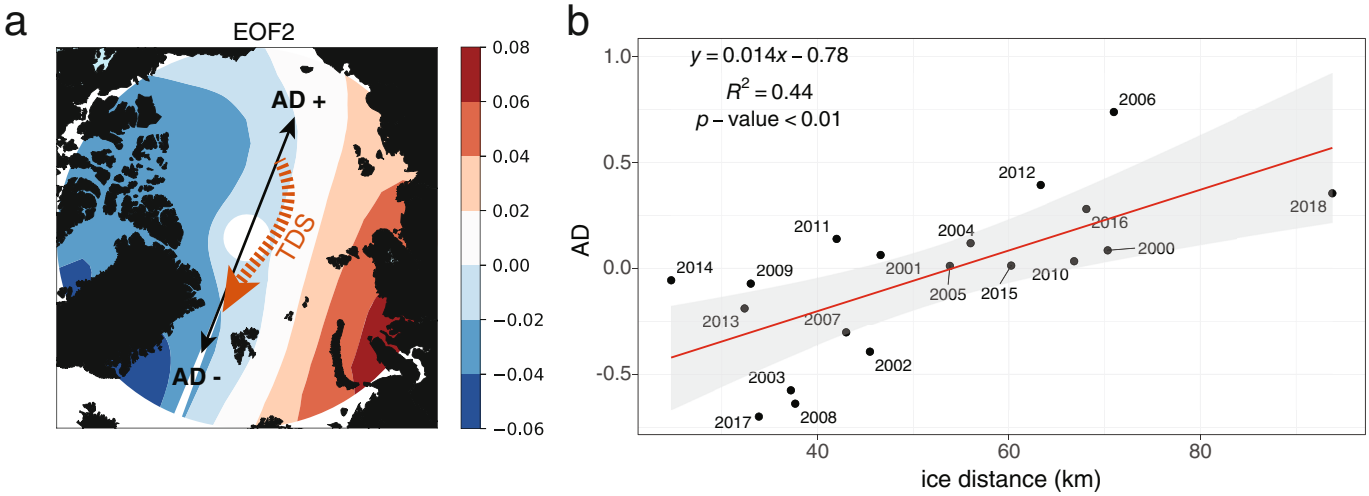

Fig. 4. (**a**) Arctic Dipole represented by the 2nd leading EOF of annual-mean sea-level pressure anomalies, combined with (**b**) a linear regression between the mean of Arctic Dipole index and sea-ice distance during the winter–spring period (January–June).

dynamic and Arctic Dipole index has been observed during the winter–spring period, confirming the strong potential role of Arctic Dipole in determining the sea-ice distance to the mooring site HG-IV during this period (Fig. 4b; $R^2 = 0.44$; p-value < 0.01).

Vertical distribution of swimmers and sinkers

Vertical distribution of zooplankton was identified by comparing the three sediment trap depths (180–280, 800–1320, and 2320–2550 m). The phenology of pteropoda collected by the upper sediment traps (i.e., maximum in fall and minimum

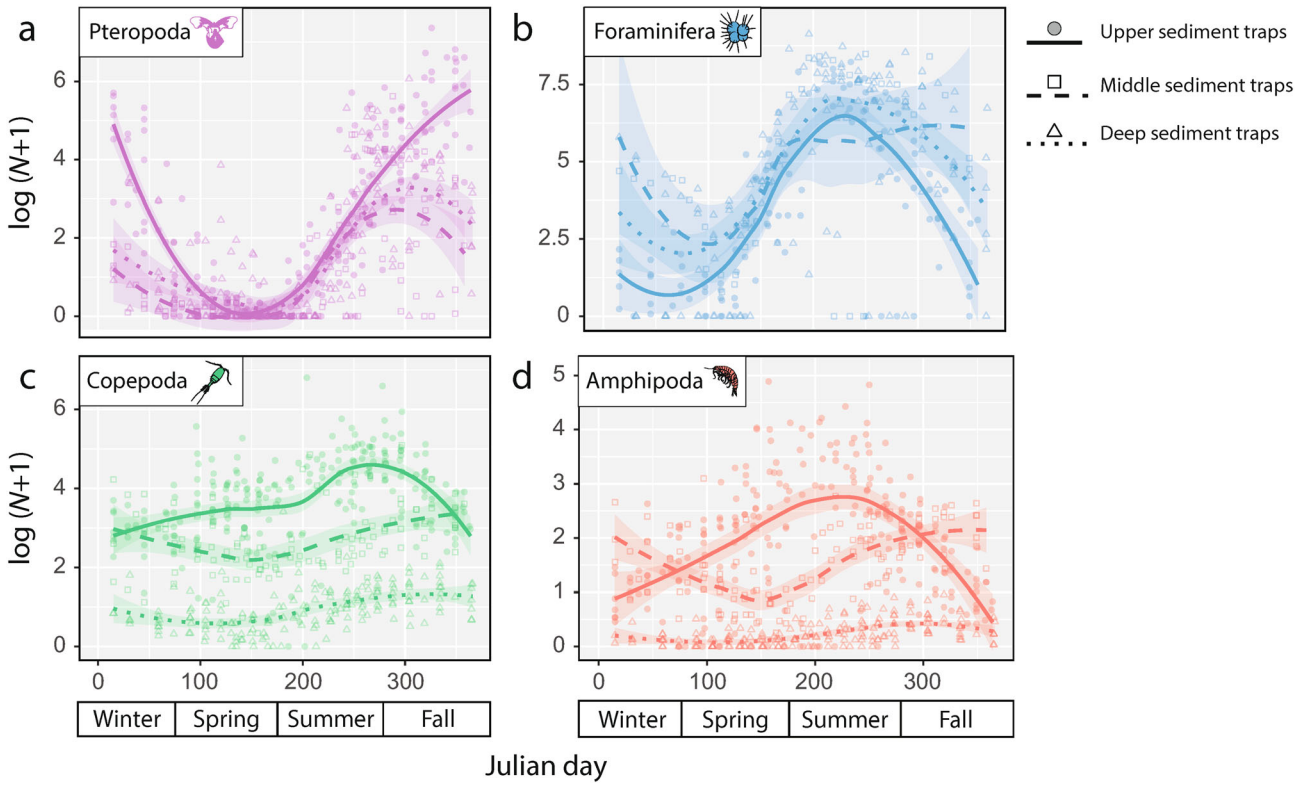

Fig. 5. Yearly pattern of pteropoda (**a**), foraminifera (**b**), copepoda (**c**), and amphipoda (**d**) log-transformed abundance in the upper (circle and full line), middle (square and dash line), and deep (triangle and point line) sediment traps at the central station of HAUSGARTEN observatory. The lines represent the average log-transformed abundance and the shaded area the 95% confidence level interval.

in spring) was similar to the deeper traps. However, high abundances were observed in deep traps compared to the middle traps but were still lower than the pteropoda abundances collected by the upper traps (Fig. 5a). Opposite to pteropoda, the seasonality of the foraminifera showed a clear seasonal shift from high occurrence during summer to low abundances during winter for all trap depths (Fig. 5b). Surprisingly, foraminifera were found with similar or sometimes higher abundances in the deeper traps compared to the upper trap. In contrast to the sinkers, the vertical seasonal distribution of the swimmers changed significantly with increasing depth. Chaetognatha and ostracoda were mainly observed in the upper sediment traps (Fig. 2) while lower numbers of individuals were recorded in the middle and deep traps (data not shown). Copepoda and amphipoda were abundant in the middle traps during fall and winter, while the upper traps showed high abundances during spring and summer (Fig. 5c,d).

Discussion

Zooplankton swimmers and sinkers—Uncertainties

It is not an easy task to distinguish between swimmers and sinkers when sorting zooplankton from sediment trap collected material. Especially when it comes to copepoda and amphipoda, it is very subjective (i.e., picker's judgment) to identify if they actively swam into the trap (swimmer) and were killed by the fixative or if they died and subsequently sank into the trap (sinker). In addition, some swimmers, called "cryptic swimmers" and mainly represented by gelatinous zooplankton, are difficult to observe and remove from the remaining material because they are transparent, fragile, or damaged during sample handling (Michaels et al. 1990). Another major swimmer-related issue is the "zooplankton product," that is, defaecation caused by the fixative in the trap and material carried with the swimmer into the trap, such as mucous nets, eggs, houses, and so on (Harbison and Gilmer 1986).

Several technics tried to resolve swimmer problems by designing specific traps (indented rotating sphere trap or screened trap; Michaels et al. 1990; Peterson et al. 1993), which limit the entrance of living organisms, or by using supravital staining (Neutral red; Ivory et al. 2014) to distinguish swimmers and carcasses. However, these approaches also showed their limits. For instance, screened traps were efficient to avoid the entrance of large zooplankton, but excluded much of the fine settling material considerably smaller than the mesh of the screen (Michaels et al. 1990).

To minimize biases, we deployed our traps below the euphotic zone where swimmers are more rare (Lee et al. 1988).

We sorted swimmers and sinkers according to the swimming ability and level of degradation of individuals. Still, zooplankton samples collected by sediment traps are at best semi-quantitative and cannot be used for quantitative ecological studies. Despite these difficulties, zooplankton collected by sediment traps still show the presence of specific groups/species as swimmers or/and sinkers and offer long time series that can be used as proxies to understand zooplankton community dynamics.

Here, we used a sediment trap time series to study temporal and spatial zooplankton dynamics in relation to long-term environmental variables in the Fram Strait. This allowed seasonal sampling of zooplankton between 2000 and 2016, which would not be possible using zooplankton net sampling due to the difficulties in accessing the Fram Strait by ship year-round, especially during the ice-covered seasons.

Environmental changes at the central station of HAUSGARTEN observatory

For being able to evaluate zooplankton dynamics in the Fram Strait, it is of great importance to understand seasonal and interannual environmental changes in the sampling area in the 1st place. The Arctic Ocean and Fram Strait are highly dynamic oceanic environments with significant spatial and temporal variabilities in sea-ice cover that can alter the phenology and composition of plankton (Ji et al. 2013; Mayot et al. 2018).

Several climatic indices have been suggested to drive the sea-ice dynamics in the Arctic (Dickson et al. 2000; Wu et al. 2006; Smedsrud et al. 2017). In our study, Arctic Dipole appeared as the dominant climatic index that controlled sea-ice extent in the Fram Strait. During a negative phase, the changes in wind circulation impacted the transpolar sea-ice drift and, thereby, the outflow of sea-ice through the Fram Strait (Smedsrud et al. 2017). In addition to atmospheric changes, the warm Atlantic inflow also limits sea-ice coverage from the south and impacts ecological and biogeochemical processes in the area.

Usually, the changing ice conditions at the central station of the HAUSGARTEN observatory lead to a clear bimodal carbon flux seasonal pattern. Both POC peaks have been linked to phytoplankton bloom, respectively, in (i) early spring, when irradiance reaches a critical threshold level through the ice and the inorganic nutrients are sufficient to sustain exponential growth of algae, and in (ii) late summer after the ice break-up. These conditions tend to promote high POC and PbSi flux as well as high concentrations of zooplankton fecal pellets at HG-IV (Lalande et al. 2013). However, during the warm Atlantic events, we observed reduced extension of sea-ice coverage, which had an impact on the annual and interannual trends in POC flux and planktonic composition (Bauerfeind et al. 2014; Nöthig et al. 2015; Soltwedel et al. 2016). By cascading effects, these disruptions may finally have consequences for the whole Arctic ecosystem and affect the highest trophic levels (Søreide et al. 2010; Leu et al. 2011).

However, it is unclear whether the increase in POC export was caused by increasing ballasting of the export organic matter via melting out of cryogenic minerals from the ice (Wollenburg et al. 2018) or by increasing biological productivity and ecological interactions at the ice edge (Nöthig et al. 2020).

Seasonal and interannual relationship between biogeochemical flux and zooplankton communities

Pteropoda and foraminifera

The abundance of pteropoda correlated significantly with the $CaCO_3$ flux, confirming the results of Bauerfeind et al. (2014) who showed that these shell-bearing animals were the main contributors to the calcium carbonate export in the Fram Strait. Pteropoda were more abundant in the Fram Strait since the 1st warm event, and since 2005/2006, the dominant species shifts from the Arctic species *Limacina helicina* to the sub-Arctic species *Limacina retroversa* (Bauerfeind et al. 2014; Busch et al. 2015). Unfortunately, the short foraminifera time series did not allow us to perform an interannual comparison, but still showed a clear seasonal pattern (i.e., maximum and minimum occurrences during the summer and winter, respectively), which was in agreement with previous studies from sediment traps and net sampling (Pados and Spielhagen 2014). The foraminiferal assemblage in the Fram Strait is dominated by the polar species *Neogloboquadrina pachyderma* and the subpolar species *Turborotalita quinqueloba* (Pados and Spielhagen 2014). Both pteropoda and foraminifera have their main habitat in the upper 200 m of the water column (Kobayashi 1974; Pados and Spielhagen 2014), but were still frequently observed at all trap depths down to 2500 m, which suggests that shells and dead animals may be an important part of the calcium carbonate and organic matter flux in the deep Fram Strait (Lalande et al. 2016). Pteropoda and foraminifera were often observed simultaneously at all trap depths, indicating a rapid downward flux at the end of the productive season (Fig. 6), and may represent an important food source for benthic organisms during the polar night (Bauerfeind et al. 2014).

Copepoda

In the Arctic Ocean and the Fram Strait, the genus *Calanus* dominates the copepoda group and is represented in terms of biomass mainly by the two natives species *Calanus glacialis* (Arctic) and *Calanus hyperboreus* (Arctic), and the North Atlantic species *Calanus finmarchicus* (sub-Arctic) (Falk-Petersen et al. 2007; Søreide et al. 2008). These three species are known to migrate vertically from the deep sea to the surface during spring, where they actively feed on phytoplankton and remain until the end of summer, when they migrate to the deep ocean for hibernation during winter (400–2000 m

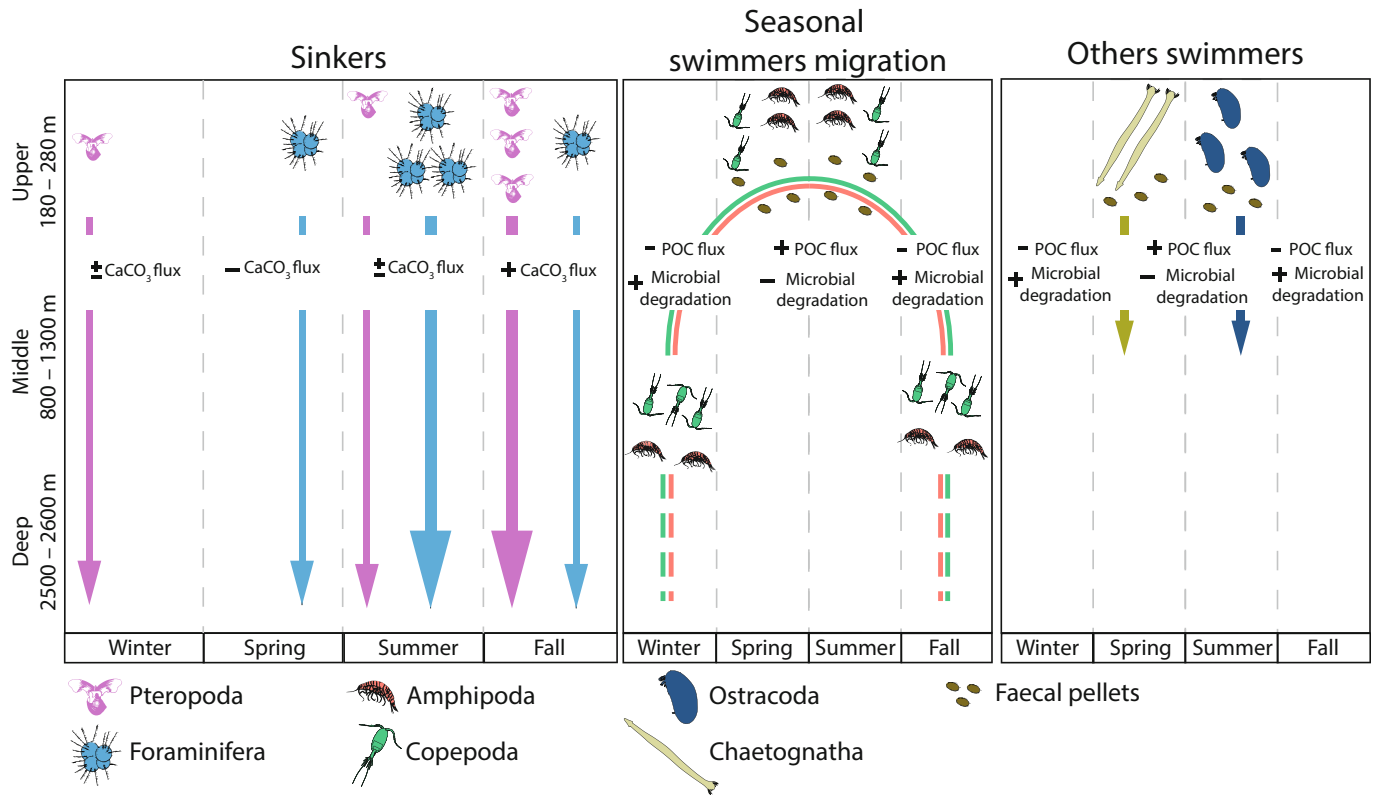

Fig. 6. Schematic overview of the seasonal and vertical swimmers and sinkers distribution observed in the upper, middle, and deep sediment traps, coupled to the biogeochemical flux patterns. The symbols −, ±, and + represent the gradient of biological processes and biogeochemical fluxes.

depending on species, stage development, and sex of the individuals; Falk-Petersen et al. 2009; Leu et al. 2011). This seasonal behavior was also observed from our sediment trap samples where copepoda abundances in the shallow traps peaked during summer when phytoplankton biomass was high (Figs. 5, 6). Conversely, we observed the highest abundances of copepoda in the middle and deep traps during winter (Figs. 5, 6). Interannually, the highest surface copepoda abundances were observed from spring to autumn from 2005 to 2013, except in 2007. During this period, the copepoda appeared in the upper traps at least 3 months earlier than in 2001, 2007, and between the years 2014 and 2016. This earlier occurrence of copepoda might be explained by the warm Atlantic inflow into the Fram Strait. For instance, previous studies showed that enhanced inflow of Altlantic water to the Fram Strait between 2004 and 2006 may have reduced the sea-ice concentration at HG-IV (Lalande et al. 2013) and potentially caused a shift from Arctic to sub-Arctic copepoda species (i.e., *C. finmarchicus*) via bio-advection (Oziel et al. 2020). Furthermore, Ershova et al. (2021) showed strong relationships between sea-ice dynamics and the life cycle of the two native Arctic copepoda *C. glacialis* and *C. hyperboreus*. Hence, between 2008 and 2013, sea-ice conditions were likely more favorable for the phenology of native Arctic copepoda, resulting in a higher abundance of Arctic compared to Atlantic species in early spring. Thus, the warm water intrusion and the concentration and extent of sea-ice seem to be the two main factors driving the copepoda phenology in the upper sediment traps. Unfortunately, the classification level used in our study cannot confirm these hypotheses and a deeper taxonomic identification must be considered.

The $\partial^{15}N$ composition of particulate organic matter increases and decreases, respectively, according to phytoplankton growth and microbial activity (Saino and Hattori 1980). Here, a gradual decrease in $\partial^{15}N$ particulate organic matter from winter to summer and consequently a strong negative correlation with the copepoda group was observed. This relationship was not surprising because high abundances of copepoda were observed in spring/summer, when particulate organic matter was less enriched in ^{15}N, likely due to the new phytoplankton growth. Additionally, this productive period promoted the formation of large fast sinking particles via aggregation, reducing the residence time of particles in the upper ocean and limiting their oxidative degradation compounds by bacterial consumption (Fig. 6).

Chaetognatha and amphipoda

Chaetognatha and amphipoda are known predators of the copepoda community (Hop et al. 2006). However, both the monthly pattern of these predators and the statistical analysis

did not show a clear correlation to the potential copepoda prey phenology in the upper sediment traps. Based on analyses of gut contents, Casanova et al. (2012) suggested that the missing relationship between chaetognatha and prey availability in observations might be explained by their ability to feed on particulate organic matter. This would support our observations of a positive correlation among chaetognatha, ice concentration, and POC flux. Chaetognatha are sensitive to climatic shifts and are good indicators of changes in water temperature (Southward 1984). As observed for copepoda, an increasing seasonal abundance of chaetognatha was observed during the warm event and the period from 2008 to 2012 that may possibly emphasize both bio-lateral advection of temperature sensitive species of both copepoda and chaetognatha and/or suggest a trophic relationship between the two zooplankton groups. It is therefore possible that the most abundant carnivorous chaetognatha species in the Fram Strait (*Eukrohnia hamata* and *Parasagitta elegans*; Hop et al. 2006) fed on both settling aggregates and copepoda (Søreide et al. 2006).

The collected amphipoda consisted of three species; *Themisto libellula* (Arctic), *Themisto abyssorum* (sub-Arctic) and the North Atlantic *Themisto compressa* (Kraft et al. 2013, 2015; Schröter et al. 2019). Even if pelagic amphipoda prey are widely diverse (Havermans et al. 2019), the three species are mainly identified as carnivorous and extensively feed on *Calanus* spp. (Kraft et al. 2015). Recently, Schröter et al. (2019) described long terms trends in abundance of *Themisto* spp. in the eastern Fram Strait between 2000 to 2014, and provided evidence for changes in the amphipoda community linked to the expanded distribution of the Atlantic hyperiid amphipoda *T. compressa*. Nevertheless, our interannual pattern showed an extremely low abundance of this group during the warm Atlantic intrusion (i.e., 2005/2006), including the appearance of the Atlantic species that was observed for the 1st time at HG-IV in July 2004 (Kraft et al. 2013). The low ice concentration during the warm event in the Fram Strait combined with the results of the RDA suggest that the amphipoda were mainly present when sea-ice was close to the sediment trap position. However, our hypothesis needs further investigation. Interestingly, the reverse abundance trends of amphipoda in the middle and deep sediment traps compared to the upper traps showed strong vertical seasonal migration from the surface to several hundred meters depth (Fig. 6), which agrees with earlier studies (Vinogradov 1999; Havermans et al. 2019). This migratory behavior, which is similar to that of the copepoda, suggests that some prey–predator relationships exist between amphipoda and copepoda.

Conclusion

By using a long time series of sediment trap collection of zooplankton we were able to identify (i) interannual, (ii) seasonal patterns, and (iii) the migration behavior of the main zooplankton organisms in the Fram Strait and relate those to environmental conditions and biogeochemical fluxes. This shows that long-term observations obtained by moored sediment traps may not only be a valuable tool to capture zooplankton dynamics but also for our understanding of biogeochemical processes and their interactions with zooplankton. This is especially true for extreme ecosystems where it is difficult to obtain seasonal and long-term data. Our results show that sea-ice coverage represents the main factor to explain biogeochemical cycles and energy transfer in marine food web changes in the Fram Strait. With the projections of earlier ice-free conditions and an even stronger warming due to enhanced inflow of Atlantic water in the future Fram Strait and Eurasian Arctic, we may be facing large changes in both zooplankton and phytoplankton communities (Forest et al. 2010). The changes in ecosystem structures, such as primary producer phenology (timing, duration, and magnitude) or physical conditions (temperature maximum), affect zooplankton population size by impacting survival, recruitment, and distribution parameters. In addition, the amount of warm Atlantic water inflow promotes northward plankton displacement and allows intrusion of species that are adapted to warmer temperatures (Vernet et al. 2019). By cascading effects, the small changes in the Arctic and sub-Arctic food chain cycle could propagate to higher trophic levels including fish, marine mammals, and seabirds (Søreide et al. 2010) and affect biogeochemical processes and carbon sequestration (Tremblay et al. 2015). For example, chaetognatha and amphipoda provide an important link to higher trophic level and are important prey for fish (e.g., capelin, cod), birds, and marine mammals (Mehlum and Gabrielsen 1993; Havermans et al. 2019). Since both chaetognatha and amphipoda were shown to be affected by sea-ice dynamics and water temperatures, the current impact of climate change on the ecosystem in the Fram Strait may have consequences for the entire food web. This highlights that understanding the causes and effects of the changes in sea-ice dynamics is still an important challenge.

Data availability statement

The data supporting the findings of this study are available in the Pangaea Database (https://www.pangaea.de/).

References

Aagaard, K., A. Foldvik, and S. Hillman. 1987. The West Spitsbergen current: Disposition and water mass transformation. J. Geophys. Res. Oceans **92**: 3778–3784. doi:10.1029/JC092iC04p03778

Barber, D. G., and others. 2015. Selected physical, biological and biogeochemical implications of a rapidly changing Arctic Marginal Ice Zone. Prog. Oceanogr. **139**: 122–150. doi:10.1016/j.pocean.2015.09.003

Bauerfeind, E., and others. 2009. Particle sedimentation patterns in the eastern Fram Strait during 2000–2005: Results

from the Arctic long-term observatory HAUSGARTEN. Deep-Sea Res. I Oceanogr. Res. Pap. **56**: 1471–1487. doi:10.1016/j.dsr.2009.04.011

Bauerfeind, E., E.-M. Nöthig, B. Pauls, A. Kraft, and A. Beszczynska-Möller. 2014. Variability in pteropod sedimentation and corresponding aragonite flux at the Arctic deep-sea long-term observatory HAUSGARTEN in the eastern Fram Strait from 2000 to 2009. J. Mar. Syst. **132**: 95–105. doi:10.1016/j.jmarsys.2013.12.006

Beszczynska-Möller, A., E. Fahrbach, U. Schauer, and E. Hansen. 2012. Variability in Atlantic water temperature and transport at the entrance to the Arctic Ocean, 1997–2010. ICES J. Mar. Sci. **69**: 852–863. doi:10.1093/icesjms/fss056

Busch, K., E. Bauerfeind, and E.-M. Nöthig. 2015. Pteropod sedimentation patterns in different water depths observed with moored sediment traps over a 4-year period at the LTER station HAUSGARTEN in eastern Fram Strait. Polar Biol. **38**: 845–859.

Carmack, E., and others. 2015. Toward quantifying the increasing role of oceanic heat in sea-ice loss in the new Arctic. Bull. Am. Meteorol. Soc. **96**: 2079–2105.

Casanova, J.-P., R. Barthelemy, M. Duvert, and E. Faure. 2012. Chaetognaths feed primarily on dissolved and fine particulate organic matter, not on prey: Implications for marine food webs. Hypotheses Life Sci. **2**: 20–29.

Cavalieri, D. J., C. L. Parkinson, P. Gloersen, and H. J. Zwally. 1996. Sea-ice concentrations from Nimbus-7 SMMR and DMSP SSM/I-SSMIS Passive Microwave Data, Version 1 [November 2018]. NASA National Snow and Ice Data Center Distributed Active Archive Center.

Cavalieri, D. J., and C. L. Parkinson. 2012. Arctic Sea-ice variability and trends, 1979–2010. Cryosphere **6**: 881–889. doi:10.5194/tc-6-881-2012

Comeau, A. M., W. K. Li, J. E. Tremblay, E. C. Carmack, and C. Lovejoy. 2011. Arctic Ocean microbial community structure before and after the 2007 record sea-ice minimum. PLos One **6**: e27492. doi:10.1371/journal.pone.0027492

Comiso, J. C., C. L. Parkinson, R. Gersten, and L. Stock. 2008. Accelerated decline in the Arctic Sea-ice cover. Geophys. Res. Lett. **35**: 35.

de Steur, L., E. Hansen, R. Gerdes, M. Karcher, E. Fahrbach, and J. Holfort. 2009. Freshwater fluxes in the East Greenland Current: A decade of observations. Geophys. Res. Lett. **36**: L23611. doi:10.1029/2009GL041278

Descamps, S., and others. 2017. Climate change impacts on wildlife in a high Arctic archipelago—Svalbard, Norway. Glob. Chang. Biol. **23**: 490–502. doi:10.1111/gcb.13381

Dickson, R., and others. 2000. The Arctic Ocean response to the North Atlantic oscillation. J. Clim. **13**: 2671–2696. doi:10.1175/1520-0442(2000)013<2671:TAORTT>2.0.CO;2

Elmendorf, S. C., and others. 2012. Global assessment of experimental climate warming on tundra vegetation: Heterogeneity over space and time. Ecol. Lett. **15**: 164–175. doi:10.1111/j.1461-0248.2011.01716.x

Enfield, D. B., A. M. Mestas-Nuñez, and P. J. Trimble. 2001. The Atlantic multidecadal oscillation and its relation to rainfall and river flows in the continental US. Geophys. Res. Lett. **28**: 2077–2080. doi:10.1029/2000GL012745

Ershova, E. A., and others. 2021. Sea-ice decline drives biogeographical shifts of key *Calanus* species in the central Arctic Ocean. Glob. Chang. Biol. **27**: 1–16.

Fahrbach, E., and others. 2001. Direct measurements of volume transports through Fram Strait. Polar Res. **20**: 217–224. doi:10.1111/j.1751-8369.2001.tb00059.x

Falk-Petersen, S., V. Pavlov, S. Timofeev, and J. R. Sargent. 2007. Climate variability and possible effects on arctic food chains: The role of *Calanus*, p. 147–166. *In* Arctic alpine ecosystems and people in a changing environment. Springer.

Falk-Petersen, S., P. Mayzaud, G. Kattner, and J. R. Sargent. 2009. Lipids and life strategy of Arctic *Calanus*. Mar. Biol. Res. **5**: 18–39. doi:10.1080/17451000802512267

Forest, A., P. Wassmann, D. Slagstad, E. Bauerfeind, E.-M. Nöthig, and M. Klages. 2010. Relationships between primary production and vertical particle export at the Atlantic-Arctic boundary (Fram Strait, HAUSGARTEN). Polar Biol. **33**: 1733–1746. doi:10.1007/s00300-010-0855-3

Fossheim, M., R. Primicerio, E. Johannesen, R. B. Ingvaldsen, M. M. Aschan, and A. V. Dolgov. 2015. Recent warming leads to a rapid borealization of fish communities in the Arctic. Nat. Clim. Change **5**: 673–677. doi:10.1038/nclimate2647

Fromentin, J.-M., and B. Planque. 1996. Calanus and environment in the eastern North Atlantic. II. Influence of the North Atlantic Oscillation on *C. finmarchicus* and *C. helgolandicus*. Mar. Ecol. Prog. Ser. **134**: 111–118. doi:10.3354/meps134111

Harbison, G., and R. Gilmer. 1986. Effects of animal behavior on sediment trap collections: Implications for the calculation of aragonite fluxes. Deep Sea Res. Part A Oceanogr. Res. Pap. **33**: 1017–1024. doi:10.1016/0198-0149(86)90027-0

Havermans, C., H. Auel, W. Hagen, C. Held, N. S. Ensor, and G. A. Tarling. 2019. Predatory zooplankton on the move: Themisto amphipods in high-latitude marine pelagic food webs, p. 51–92. *In* Advances in marine biology. Elsevier.

Hop, H., and others. 2006. Physical and biological characteristics of the pelagic system across Fram Strait to Kongsfjorden. Prog. Oceanogr. **71**: 182–231. doi:10.1016/j.pocean.2006.09.007

Hurrell, J. W. 1995. Decadal trends in the North Atlantic oscillation: Regional temperatures and precipitation. Science **269**: 676–679. doi:10.1126/science.269.5224.676

Ivory, J. A., K. W. Tang, and K. Takahashi. 2014. Use of Neutral Red in short-term sediment traps to distinguish between zooplankton swimmers and carcasses. Mar. Ecol. Prog. Ser. **505**: 107–117. doi:10.3354/meps10775

Ji, R., M. Jin, and Ø. Varpe. 2013. Sea-ice phenology and timing of primary production pulses in the Arctic Ocean. Glob. Chang. Biol. **19**: 734–741. doi:10.1111/gcb.12074

Kelley, D., C. Richards, and C. Layton. 2018. The oce package, p. 91–101. *In* Oceanographic analysis with R. Springer.

Kiørboe, T., and A. W. Visser. 1999. Predator and prey perception in copepods due to hydromechanical signals. Mar. Ecol. Prog. Ser. **179**: 81–95.

Knauer, G. A., J. H. Martin, and K. W. Bruland. 1979. Fluxes of particulate carbon, nitrogen, and phosphorus in the upper water column of the northeast Pacific. Deep Sea Res. Part A Oceanogr. Res. Pap. **26**: 97–108.

Kobayashi, H. 1974. Growth cycle and related vertical distribution of the thecosomatous pteropod *Spiratella* ("*Limacina*") *helicina* in the central Arctic Ocean. Mar. Biol. **26**: 295–301. doi:10.1007/BF00391513

Kraft, A., J. Berge, Ø. Varpe, and S. Falk-Petersen. 2013. Feeding in Arctic darkness: Mid-winter diet of the pelagic amphipods *Themisto abyssorum* and *T. libellula*. Mar. Biol. **160**: 241–248. doi:10.1007/s00227-012-2065-8

Kraft, A., M. Graeve, D. Janssen, M. Greenacre, and S. Falk-Petersen. 2015. Arctic pelagic amphipods: Lipid dynamics and life strategy. J. Plankton Res. **37**: 790–807.

Lalande, C., E. Bauerfeind, E.-M. Nöthig, and A. Beszczynska-Möller. 2013. Impact of a warm anomaly on export fluxes of biogenic matter in the eastern Fram Strait. Prog. Oceanogr. **109**: 70–77. doi:10.1016/j.pocean.2012.09.006

Lalande, C., E.-M. Nöthig, E. Bauerfeind, K. Hardge, A. Beszczynska-Möller, and K. Fahl. 2016. Lateral supply and downward export of particulate matter from upper waters to the seafloor in the deep eastern Fram Strait. Deep-Sea Res. I Oceanogr. Res. Pap. **114**: 78–89. doi:10.1016/j.dsr.2016.04.014

Lee, C., S. G. Wakeham, and J. I. Hedges. 1988. The measurement of oceanic particle flux-are "swimmers" a problem? Oceanography **1**: 34–36. doi:10.5670/oceanog.1988.06

Legendre, P., and L. F. Legendre. 2012. Numerical ecology, 3rd ed. Elsevier.

Leu, E., J. Søreide, D. Hessen, S. Falk-Petersen, and J. Berge. 2011. Consequences of changing sea-ice cover for primary and secondary producers in the European Arctic shelf seas: Timing, quantity, and quality. Prog. Oceanogr. **90**: 18–32. doi:10.1016/j.pocean.2011.02.004

Lindsay, R., and A. Schweiger. 2015. Arctic Sea-ice thickness loss determined using subsurface, aircraft, and satellite observations. Cryosphere **9**: 269–283. doi:10.5194/tc-9-269-2015

Loeng, H. 1991. Features of the physical oceanographic conditions of the Barents Sea. Polar Res. **10**: 5–18.

Makabe, R., and others. 2010. Regional and seasonal variability of zooplankton collected using sediment traps in the southeastern Beaufort Sea, Canadian Arctic. Polar Biol. **33**: 257–270. doi:10.1007/s00300-009-0701-7

Maslowski, W., D. Marble, W. Walczowski, U. Schauer, J. L. Clement, and A. J. Semtner. 2004. On climatological mass, heat, and salt transports through the Barents Sea and Fram Strait from a pan-Arctic coupled ice-ocean model simulation. J. Geophys. Res. Oceans **109**: C03032. doi:10.1029/2001JC001039

Mayot, N., and others. 2018. Assessing phytoplankton activities in the seasonal ice zone of the Greenland Sea over an annual cycle. J. Geophys. Res. Oceans **123**: 8004–8025. doi:10.1029/2018JC014271

Mehlum, F., and G. Gabrielsen. 1993. The diet of high-arctic seabirds in coastal and ice-covered, pelagic areas near the Svalbard archipelago. Polar Res. **12**: 1–20. doi:10.1111/j.1751-8369.1993.tb00417.x

Michaels, A. F., M. W. Silver, M. M. Gowing, and G. A. Knauer. 1990. Cryptic zooplankton "swimmers" in upper ocean sediment traps. Deep Sea Res. Part A Oceanogr. Res. Pap. **37**: 1285–1296. doi:10.1016/0198-0149(90)90043-U

Nöthig, E.-M., and others. 2015. Summertime plankton ecology in Fram Strait—A compilation of long-and short-term observations. Polar Res. **34**: 23349. doi:10.3402/polar.v34.23349

Nöthig, E.-M., and others. 2020. Summertime chlorophyll a and particulate organic carbon standing stocks in surface waters of the Fram Strait and the Arctic Ocean (1991–2015). Front. Mar. Sci. **7**: 1-15. doi:10.3389/fmars.2020.00350

Oziel, L., and others. 2020. Faster Atlantic currents drive poleward expansion of temperate phytoplankton in the Arctic Ocean. Nat. Commun. **11**: 1–8.

Pados, T., and R. F. Spielhagen. 2014. Species distribution and depth habitat of recent planktic foraminifera in Fram Strait. Arctic Ocean. Polar Res. **33**: 22483.

Peterson, M., P. Hernes, D. Thoreson, J. Ifedges, C. Lee, and S. Wakeham. 1993. Field evaluation of a valved sediment trap. Limnol. Oceanogr. **38**: 1741–1761. doi:10.4319/lo.1993.38.8.1741

Polyakov, I. V., and others. 2017. Greater role for Atlantic inflows on sea-ice loss in the Eurasian Basin of the Arctic Ocean. Science **356**: 285–291. doi:10.1126/science.aai8204

Polyakov, I. V., and others. 2020. Borealization of the Arctic Ocean in response to anomalous advection from sub-Arctic seas. Front. Mar. Sci. **7**: 491.

Pörtner, H., and others 2019. IPCC special report on the ocean and cryosphere in a changing climate. IPCC Intergovernmental Panel on Climate Change: Geneva, Switzerland, **1**(3).

Saino, T., and A. Hattori. 1980. 15N natural abundance in oceanic suspended particulate matter. Nature **283**: 752–754. doi:10.1038/283752a0

Schröter, F., and others. 2019. Pelagic amphipods in the Eastern Fram Strait with continuing presence of *Themisto compressa* based on sediment trap time series. Front. Mar. Sci. **6**: 311.

Smedsrud, L. H., A. Sirevaag, K. Kloster, A. Sorteberg, and S. Sandven. 2011. Recent wind driven high sea-ice area export in the Fram Strait contributes to Arctic Sea-ice decline. Cryosphere **5**: 821–829. doi:10.5194/tc-5-821-2011

Smedsrud, L. H., M. H. Halvorsen, J. C. Stroeve, R. Zhang, and K. Kloster. 2017. Fram Strait sea-ice export variability and September Arctic Sea-ice extent over the last 80 years. Cryosphere **11**: 65–79. doi:10.5194/tc-11-65-2017

Soltwedel, T., and others. 2016. Natural variability or anthropogenically-induced variation? Insights from 15 years of multidisciplinary observations at the arctic marine LTER site HAUSGARTEN. Ecol. Indic. **65**: 89–102. doi:10.1016/j.ecolind.2015.10.001

Søreide, J. E., H. Hop, M. L. Carroll, S. Falk-Petersen, and E. N. Hegseth. 2006. Seasonal food web structures and sympagic–pelagic coupling in the European Arctic revealed by stable isotopes and a two-source food web model. Prog. Oceanogr. **71**: 59–87. doi:10.1016/j.pocean.2006.06.001

Søreide, J. E., and others. 2008. Seasonal feeding strategies of Calanus in the high-Arctic Svalbard region. Deep-Sea Res. II Top. Stud. Oceanogr. **55**: 2225–2244. doi:10.1016/j.dsr2.2008.05.024

Søreide, J. E., E. V. Leu, J. Berge, M. Graeve, and S. Falk-Petersen. 2010. Timing of blooms, algal food quality and *Calanus glacialis* reproduction and growth in a changing Arctic. Glob. Chang. Biol. **16**: 3154–3163.

Southward, A. 1984. Fluctuations in the "indicator" chaetognaths *Sagitta elegans*. Oceanol. Acta **7**: 229–239.

Tesi, T., and others. 2021. Rapid Atlantification along the Fram Strait at the beginning of the 20th century. Sci. Adv. **7**: eabj2946. doi:10.1126/sciadv.abj2946

Tokuhiro, K., and others. 2019. Seasonal phenology of four dominant copepods in the Pacific sector of the Arctic Ocean: Insights from statistical analyses of sediment trap data. Polar Sci. **19**: 94–111. doi:10.1016/j.polar.2018.08.006

Tremblay, J.-É., and others. 2015. Global and regional drivers of nutrient supply, primary production and CO_2 drawdown in the changing Arctic Ocean. Prog. Oceanogr. **139**: 171–196. doi:10.1016/j.pocean.2015.08.009

Vernet, M., I. H. Ellingsen, L. Seuthe, D. Slagstad, M. R. Cape, and P. A. Matrai. 2019. Influence of phytoplankton advection on the productivity along the Atlantic Water Inflow to the Arctic Ocean. Front. Mar. Sci. **6**: 583.

Vinogradov, G. M. 1999. Deep-sea near-bottom swarms of pelagic amphipods Themisto: Observations from submersibles. Sarsia **84**: 465–467.

Willis, K., F. Cottier, S. Kwasniewski, A. Wold, and S. Falk-Petersen. 2006. The influence of advection on zooplankton community composition in an Arctic fjord (Kongsfjorden, Svalbard). J Mar. Syst. **61**: 39–54. doi:10.1016/j.jmarsys.2005.11.013

Wollenburg, J., and others. 2018. Ballasting by cryogenic gypsum enhances carbon export in a *Phaeocystis* under-ice bloom. Sci Rep **8**: 1–9.

Wu, B., J. Wang, and J. E. Walsh. 2006. Dipole anomaly in the winter Arctic atmosphere and its association with sea-ice motion. J. Clim. **19**: 210–225. doi:10.1175/JCLI3619.1

Zamani, B., T. Krumpen, L. H. Smedsrud, and R. Gerdes. 2019. Fram Strait sea-ice export affected by thinning: Comparing high-resolution simulations and observations. Clim. Dyn. **53**: 1–14.

Acknowledgments

The authors thank C. Lorenzen and E. Bonk (Alfred Wegener Institute Helmholtz Centre for Polar and Marine Research) for lab assistance and the tedious work of swimmers picking. We also thank all the helpers picking out swimmers from the traps. The authors also would like to thank the AWI Physical Oceanography section, the AWI Deep Sea group and captains and crews of RV Polarstern and RV Maria S. Merian for their support during service of the HAUSGARTEN Observatory. This study was funded by the German Federal Ministry of Education and Research (project: 03F0629A) and the "Polar System and its effects on the Ocean Floor (POSY)" project. The International Science Program also supported this research for Integrative Research in Earth Systems. This work was conducted in the framework of the HGF Infrastructure Program FRAM of the Alfred-Wegener-Institute Helmholtz Center for Polar and Marine Research. Additional funding came from the HGF Young Investigator Group SeaPump "Seasonal and regional food web interactions with the biological pump": VH-NG-1000 and the DFG-Research Center/Cluster of Excellence "The Ocean Floor—Earth's Uncharted Interface": EXC-2077-390741603. This work was also part of the Helmholtz Program "Changing Earth—Sustaining our Future" supported by the Helmholtz Program-Orientated Funding (POF IV) to topic 6 (Marine Life) and the subtopics 6.1 (Future Ecosystem Functionality) and 6.3 (The Future Biological Carbon Pump). M. Seifert was supported by funding from the Initiative and Networking Fund of the Helmholtz Association (Helmholtz Young Investigator Group Marine Carbon and Ecosystem Feedbacks in the Earth System [MarESys], grant number VH-NG-1301) during the manuscript preparation. Open Access funding enabled and organized by Projekt DEAL.

Conflict of Interest

None declared.

Submitted 30 August 2021
Revised 04 March 2022
Accepted 06 July 2022

Guest editor: Sarah A. Woodin